AD-A037 218 DEFENCE RESEARCH ESTABLISHMENT VALCARTIER (QUEBEC) F/G 20/5
STEADY STATE THERMAL BLOOMING OF MULTIPULSE LASER BEAMS,(U)
FEB 77 L R BISSONNETTE

UNCLASSIFIED DREV-R-4067/77 NL

1 OF 1
AD
AD37218

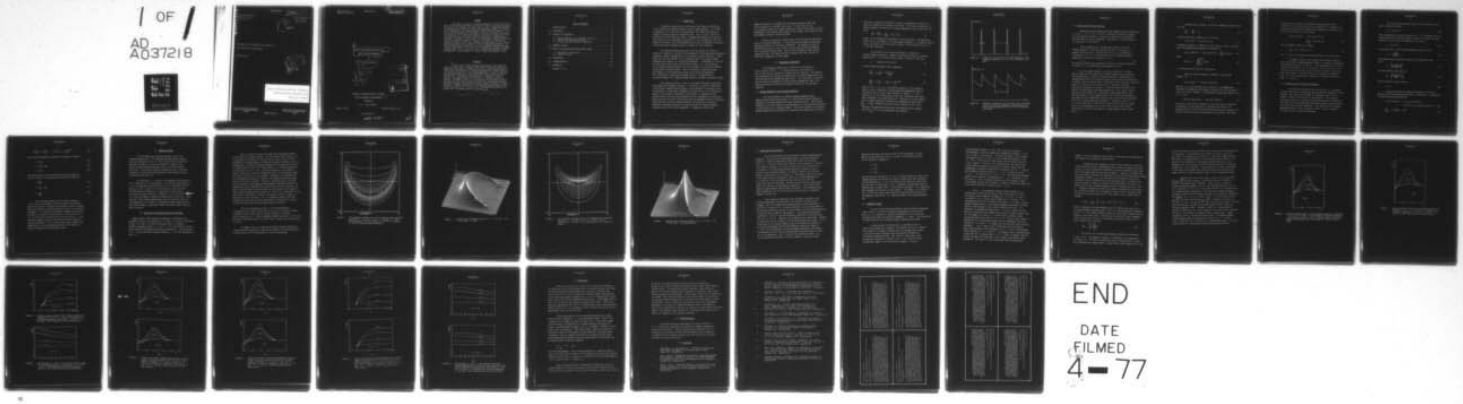

END

DATE
FILMED
4-77

UNCLASSIFIED

CRDV RAPPORT 4067/77
DOSSIER: 3634C-004
FÉVRIER 1977

DREV REPORT 4067/77
FILE: 3634C-004
FEBRUARY 1977

3 NW

STEADY STATE THERMAL BLOOMING OF MULTIPULSE LASER BEAMS

L.R. Bissonnette

Centre de Recherches pour la Défense
Defence Research Establishment
Valcartier, Québec

BUREAU - RECHERCHE ET DEVELOPPEMENT
MINISTERE DE LA DEFENSE NATIONALE
CANADA

NON CLASSIFIÉ

RESEARCH AND DEVELOPMENT BRANCH
DEPARTMENT OF NATIONAL DEFENCE
CANADA

CRDV R-4067/77
DOSSIER: 3634C-004

UNCLASSIFIED

(14) DREV-R-4067/77
FILE: 3634C-004

(6)

STEADY STATE THERMAL BLOOMING OF MULTIPULSE LASER BEAMS,

by

(10) L.R. Bissonnette

(11) 7 Feb 77

(12) 36 p.

CENTRE DE RECHERCHES POUR LA DEFENSE
DEFENCE RESEARCH ESTABLISHMENT
VALCARTIER
Tel: (418) 844-4271
Québec, Canada

February/février 1977

NON CLASSIFIE

404 945

1B

RESUME

On étudie, à l'aide de solutions numériques, l'état stationnaire de la défocalisation thermique d'un faisceau laser à impulsions multiples soumis à un vent latéral. On trouve, pour un taux d'impulsions favorable, une augmentation de 100% de l'intensité maximale par rapport au faisceau qui se propagerait sans déformation mais avec absorption linéaire. La valeur correspondante du gain exprimé en terme de l'intensité moyenne sur la surface de la cible qui reçoit 85% de la puissance totale est de 40%. Trois paramètres de similitude suffisent pour définir complètement le problème: le nombre κ qui est égal à la réciproque du nombre d'impulsions transmises pendant le temps de transit de l'air dans le faisceau, le nombre de Fresnel F basé sur la longueur caractéristique de l'interaction absorption-intensité et le nombre γ relié à l'absorption linéaire. Une étude paramétrique en fonction de ces trois paramètres démontre que des conditions optimales de gain dans le cas d'un faisceau gaussien collimaté existent pour: $0.8 \leq \kappa \leq 1.0$ et $F \geq 20$. L'amplification décroît généralement avec l'accroissement de γ mais de façon peu sensible. (NC)

ABSTRACT

Steady state thermal blooming of multipulse laser beams subjected to cross winds is studied in the light of numerical solutions. Enhancement resulting in a 100% increase of the peak irradiance with respect to the non-bloomed but linearly absorbed beam is demonstrated at the optimal pulsing rate. The corresponding gain in terms of spatially averaged power density over the target area containing 85% of total power is 40%. A parametric study is made as a function of three similarity parameters which are sufficient to completely define the problem: the number κ which is the reciprocal of the number of pulses per flow time, the Fresnel number F based on the absorption-irradiance interaction length scale and the absorption number γ related to linear depletion. Optimal conditions for a collimated Gaussian beam are shown to exist for $0.8 \leq \kappa \leq 1.0$ and $F \geq 20$. Intensification generally decreases with increasing γ but only slightly. (U)

Kappa — gamma — gamma — approximately less than — approximately greater than

TABLE OF CONTENTS

1.0 INTRODUCTION

Atmospheric applications of high-power laser beams are subjected to the nonlinear distorting mechanism called thermal blooming. As a result of absorption of a fraction of the beam power, the enthalpy of the air is slightly increased along the propagation path. This, in turn, alters the distribution of the refractive index. Although these changes are relatively small owing to the low absorption coefficient of the atmosphere at the wavelengths of interest, they can nevertheless give rise to significant distortion of the laser beam irradiance profile at ranges of a few kilometers.

The thermal blooming process has been the subject of extensive theoretical studies but, because of the complexity of the modelling differential equations, computer programs had to be developed to obtain solutions. Experiments were mostly performed in the laboratory where the thermal blooming phenomenon was enhanced in a controlled atmosphere. A comprehensive review of the work done on this subject may be found in Refs. 1-5. Investigations on the thermal blooming process were also undertaken at the Defence Research Establishment Valcartier (DREV). Refs. 6-8 present a theoretical model with emphasis on the definition and the use of similarity parameters. Ref. 9 describes a simulation experiment and Ref. 10 summarizes the principal features of a computer program based on the DREV's theoretical model.

This report describes a study of the thermal blooming of multipulse laser beams using computer solutions. A reduction, or even an elimination, of the adverse thermal blooming effects can be expected if high-power lasers are operated in a multipulse configuration rather than in a cw configuration. Indeed, if the energy is delivered to the target in a sequence of short powerful bursts, the heat energy deposited in the atmosphere by the previous pulses may have time to be carried away from the propagation path by conduction, free convection or forced convection before the next pulse is emitted. Therefore, favourable conditions of application may be obtained through a judicious choice of the laser parameters. A parametric study of the

computer solutions is performed for a collimated Gaussian laser beam in the presence of a constant cross wind. It shows that not only can the adverse effects of thermal blooming be eliminated but that an actual enhancement of the average power density on the target, with respect to the non-blooming situation, can be achieved.

Section 2.0 presents a brief review of the theoretical background and of the working hypotheses. It also discusses the model of multipulse heating and defines the similarity parameters. The numerical method is described in Section 3.0 and Section 4.0 gives and analyzes the results for a collimated Gaussian beam. The work was performed at DREV between January and June 1976 under PCN 34C04 (formerly PCN 07E04, Project No. 97-01-38), Propagation of Laser Beams.

2.0 THEORETICAL BACKGROUND

The propagation model used to construct our algorithm is fully described in Ref. 7. It differs from more conventional models in that the wave equation is broken into two equations: one equation for the geometrical rays and one equation for the complex amplitude of the field defined on the geometrical phase front. This separation is exact and has the practical advantage of allowing longer propagation steps in the numerical solution of the finite difference version of the governing equations.

2.1 Working Hypotheses and Governing Equations

Our study examines the thermal blooming phenomenon under dominant forced convection cooling, i.e. when the heat energy supplied by absorption is totally balanced by forced convection losses. The velocity component of the wind (and/or of the beam motion) in the direction transverse to the optical axis is assumed constant. Only linear changes in the thermodynamic properties of the medium are considered and compressibility effects

and kinetic cooling are neglected. Finally, longitudinal derivatives are neglected compared with crosswise derivatives. Under these conditions, the medium equations are reduced to a single temperature equation which has the form:

$$\frac{\partial\theta}{\partial t} + \frac{W\partial\theta}{\partial y} = \frac{\alpha}{\rho_o C_p} \quad I(x,y,z;t), \tag{1}$$

where θ is the temperature fluctuation, W the wind speed, α the absorption coefficient of the medium at the laser beam wavelength, ρ_o the ambient density and C_p the specific heat at constant pressure of the medium and $I(x,y,z;t)$ is the beam irradiance.

We consider a laser source pulsating at a single and constant angular frequency ω, neglect polarization and make the paraxial approximation. If the scalar electric field is written in the form:

$$E = A\exp[jk(z+\phi)-\tfrac{1}{2}\alpha z-j\omega t], \tag{2}$$

the wave equation becomes, after separation:

$$\left(\frac{\partial}{\partial z} + \underset{\sim}{V}.\nabla_t\right)\underset{\sim}{V} = \nabla_t\frac{(n-n_o)}{n_o}, \tag{3}$$

$$\left(\frac{\partial}{\partial z} + \underset{\sim}{V}.\nabla_t\right)A = -\tfrac{1}{2}A\nabla_t.\underset{\sim}{V} + \frac{j}{2k}\nabla_t{}^2A, \tag{4}$$

where $j=\sqrt{-1}$, $\underset{\sim}{V} = \nabla_t\phi$, ∇_t is the gradient operator in the transverse plane, n and n_o respectively the perturbed and unperturbed index of refraction, and k the wave number defined as follows: $k = n_o\omega/c$. Equation (3) is the eikonal equation and thus $\underset{\sim}{V}$ represents the vector angle subtended by the geometrical rays. Equation (4) is the equation for the complex amplitude A defined on the geometrical phase front: $\left(\frac{\partial}{\partial z} + \underset{\sim}{V}.\nabla_t\right)$ indicates derivation along a geometrical ray, $\frac{1}{2}A\nabla_t.\underset{\sim}{V}$ represents the geometrical effects of the converging and diverging rays and $\frac{j}{2k}\nabla_t{}^2A$ is the diffractional contribution.

FIGURE 1a - Schematic illustration of the time evolution of the irradiance function I(x,y,z;t) of a multipulse laser beam.

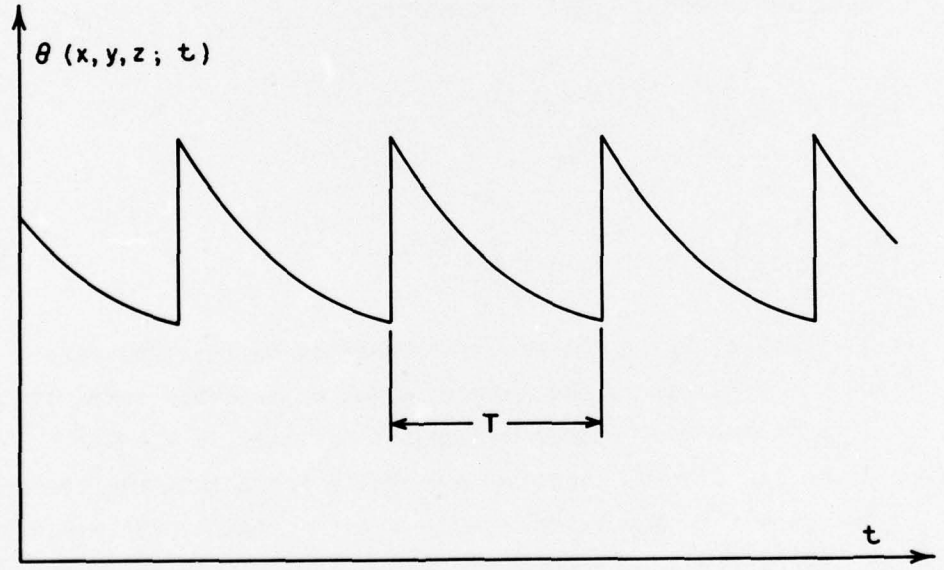

FIGURE 1b - Schematic illustration of the steady state time evolution of the periodic temperature distribution that results from the heating of the air by a multipulse laser beam.

2.2 Steady State Multipulse Heating

Multipulse thermal blooming has been studied at other laboratories e.g. Refs. 2, 3, 4, 5, 11, 12 and 13. However, the solution we propose for the temperature profile is written in a somewhat more convenient form that does not involve summation. Therefore it is worth reviewing its derivation in some details.

We are searching for a steady state solution to the temperature equation (1) when the forcing function I is a periodic sequence of short pulses. The function $I(x,y,z;t)$ is schematically illustrated in Fig. 1a. The pulse duration b is assumed negligible compared with the period of pulsation T, i.e.:

$$b \ll T. \tag{5}$$

The resulting steady state temperature solution is a periodic function of period T; it is schematically represented in Fig. 1b.

For the present purpose, we restrict ourselves to a propagation regime in which single-pulse thermal blooming can be neglected. This approximation is valid if the pulse duration is smaller than the thermalization time of the molecular energy levels excited by absorption, or smaller than the transit time of sound waves across the beam. Typically, these time scales are of the order of 1 ms. Moreover, the incompressibility hypothesis of Section 2.1 requires that the period of pulsation T be much longer than these characteristic time scales, which is consistent with relation (5). Physically, these approximations mean that the properties of the medium seen by the m^{th} pulse are completely determined by the incompressible heating that results from the absorption of the (m-1) pulses which have preceded it. Therefore, since $b \ll T$, it is clear from Figs. 1a and 1b that we need only to solve the temperature level attained just prior to the sharp increase that follows the arrival of the m^{th} pulse, where m is large enough to have steady state.

Between pulses, equation (1) for the temperature profile takes the form:

$$\frac{\partial\theta}{\partial t} + \frac{W\partial\theta}{\partial y} = 0. \tag{6}$$

A general solution to equation (6) is given by:

$$\theta[x,y,z;t] = \theta[x,y-W(t-t_o),z]. \tag{7}$$

Integrating equation (1) between $t = mT-b/2$ and $t = mT+b/2$, we obtain under the approximation expressed by relation (5):

$$\theta[x,y,z;mT+b/2] - \theta[x,y,z;mT-b/2] = \frac{\alpha}{\rho_o C_p} D[x,y,z] , \tag{8}$$

where

$$D[x,y,z] = \int_{mT-b/2}^{mT+b/2} I[x,y,z;t]dt \tag{9}$$

is the energy density profile of each pulse.

Since the overall solution is periodic, we have from equation (7):

$$\theta[x,y,z;mT+\tau] = \theta[x,y-W\tau,z;mT+b/2], \tag{10}$$

where $\frac{b}{2} \leq \tau \leq T-\frac{b}{2}$ and where $\theta[x,y,z;mT+b/2]$ is the temperature distribution immediately following the firing of the m^{th} pulse which serves as initial condition. In particular, we have from equation (10) at $\tau = T-b/2$:

$$\theta[x,y,z;(m+1)T-b/2] = \theta[x,y-WT,z;mT+b/2], \tag{11}$$

where $Wb/2$ in the spatial coordinate of the right-hand side function of equation (11) was neglected in accordance with relation (5). Replacing $(m+1)T$ by mT in the left-hand side function of equation (11), which is justified since the solution for θ is periodic, and using

equation (8) to evaluate the temperature jump between (mT-b/2) and (mT+b/2) in the right-hand side of equation (11), we obtain the following solution for the steady state temperature distribution just prior to the arrival of the m^{th} pulse:

$$\theta[x,y,z;mT-b/2] = \theta[x,y-WT,z;mT-b/2] + \frac{\alpha}{\rho_o C_p} D[x,y-WT,z], \tag{12}$$

and the boundary condition is simply:

$$\lim_{y\to-\infty} \theta[x,y,z;mT-b/2] = 0. \tag{13}$$

The $(-\infty)$- limit is actually the upwind boundary of the laser beam.

In summary, equation (12) together with boundary condition (13) constitutes a simple recurrence formula to compute the temperature distribution seen by the m^{th} pulse. In the approximation of no single-pulse thermal blooming, this is sufficient to solve the steady state average irradiance distribution of repetitively pulsed, high average power laser beams. Note that solution (12) contains no summation over the (m-1) earlier pulses in contrast with expressions given in Refs. 3, 11 and 12.

2.3 Scaling Laws and Similarity Parameters

For numerical calculations to be practical, it is important to define and use the scaling laws and the similarity parameters of the problem. This minimizes the number of parameters that have to be varied to obtain a full picture of the situation. The technique essentially consists in writing the governing equations in dimensionless form and the non-dimensional parameters emerging from the process constitute the similarity parameters. This analysis for the present propagation model is fully described in Refs. 7-8 and, therefore, the results will be simply recalled here.

The time average irradiance profile of the multipulse laser beam is defined as follows:

$$\langle I \rangle_t = AA^* e^{-\alpha z}, \tag{14}$$

where the amplitude A satisfies equation (4). If P designates the time average power and a, some representative radius of the beam, the characteristic scale for the wave amplitude A is given by:

$$A_c = (P/\pi a^2)^{\frac{1}{2}}, \tag{15}$$

the characteristic scale for the temperature variation θ by:

$$\theta_c = \frac{\alpha P T}{\rho_o C_p \pi a^2}, \tag{16}$$

the characteristic scale for the angle of the geometrical rays $\underset{\sim}{V}$ by:

$$\delta_c = \left\{ \frac{\sigma \alpha P}{\pi \rho_o C_p n_o a W} \right\}^{\frac{1}{2}}, \tag{17}$$

the longitudinal length scale by:

$$\ell_p = \left\{ \frac{\pi \rho_o C_p n_o a^3 W}{\sigma \alpha P} \right\}^{\frac{1}{2}} \tag{18}$$

and the crosswise length scale by:

$$\ell_c = a. \tag{19}$$

Using the scaling laws defined by equations (15-19) and denoting the non-dimensional functions by a superscript ', one obtains the following governing equations:

$$\theta'[\xi,\zeta,\eta;mT-b/2] = \theta'[\xi,\zeta-2\kappa,\eta;mT-b/2] + (A'A'^*)\,[\xi,\zeta-2\kappa,\eta;mT-b/2].\exp(-\gamma\eta), \tag{20}$$

$$\left(\frac{\partial}{\partial \eta} + \underset{\sim}{V}'.\nabla_t' \right) \underset{\sim}{V}' = \nabla_t' \theta', \tag{21}$$

$$\left(\frac{\partial}{\partial \eta} + \underset{\sim}{V}'.\nabla_t'\right) A' = -\tfrac{1}{2}A'\nabla_t'.\underset{\sim}{V}' + \frac{j}{2F}\nabla_t'^2 A' \ , \tag{22}$$

where the non-dimensional variables are defined as follows:

$$\eta = z/\ell_p, \tag{23}$$

$$\xi = x/\ell_c, \text{ and} \tag{24}$$

$$\zeta = y/\ell_c. \tag{25}$$

From examination of the non-dimensional governing equations (20-22), we have the following three similarity parameters:

$$\kappa = \frac{WT}{2a} \ , \tag{26}$$

$$\gamma = \alpha\ell_p \ , \text{ and} \tag{27}$$

$$F = \frac{ka^2}{\ell_p} \ . \tag{28}$$

For a collimated beam of given initial geometry, κ, γ and F are the only numbers that are required to completely specify the problem of steady state multipulse thermal blooming under the conditions and approximations listed in the preceding paragraphs. κ is called the displacement number which gives an estimate of the number of beam diameters a heated particle of air is transversely drifted between successive pulses, γ is the absorption number related to the effect of overall linear depletion and finally F is the Fresnel number which measures the magnitude of cw thermal blooming distortion with respect to natural divergence or diffractional effects.

3.0 NUMERICAL METHOD

The non-dimensional governing equations (20-22) are integrated numerically. The algorithm and computational details are fully described in Ref. 10. The system of finite difference equations is implicit, and the nonlinearity in equation (21) and the coupling between equations (20-22) are solved through iterations. The predictor-corrector approach of Ref. 10 has been replaced by a simpler and unconditionally stable method of alternating directions (Ref. 14).

The functions θ' , V'_ζ and A' are symmetric with restect to the ζ- axis while V'_ξ is antisymmetric. All functions are defined on a 30 x 60 homogeneous grid and the mesh size is adjustable at each propagation step to optimize the utilization of the grid points. The longitudinal increment $\Delta\eta$ is recalculated at each step to satisfy the accuracy criterion. Typically, $\Delta\eta$ is of the order of 0.1, which corresponds in practical applications to 100-300 m. These relatively long forward computational steps are possible since the wave amplitude A is defined on the geometrical phase front which, at high Fresnel numbers, constitutes almost the entire thermal blooming phase distortion.

4.0 RESULTS FOR COLLIMATED GAUSSIAN LASER BEAMS

Sample results of the predicted irradiance distribution of an originally Gaussian laser beam with F = 20 and γ = 0.45 are illustrated in Figs. 2-5. Figs. 2-3 give the continuous wave (cw) thermal blooming irradiance profile (κ = 0) at η = 1.15 in the form of iso-irradiance contours and isometric projection respectively. Similar results at η = 1.12 for multipulse thermal blooming (κ = 0.8) are reproduced in Figs. 4-5.

Figs. 2-5 show that there are significant differences between cw and multipulse thermal blooming. The time average peak irradiance of the multipulse distribution is nearly twice as large as that of the cw distribution and approximately 1.9 times the maximum irradiance of the non-bloomed beam. The point of maximum irradiance of the multipulse pattern is located almost on the line of sight whereas it is displaced upwind by 0.9 beam radius in the cw case. The beam divergence in the direction normal to the wind is near the diffraction limit in the multipulse regime but exceeds this limit in the cw regime. Physically, the absorbed heat in the multipulse situation is shifted on the downwind side of the beam when the m^{th} pulse is emitted. Therefore, the upwind half of the beam sees no refractive index gradient and propagates unperturbed whereas the downwind half sees a gradient which tends to bend its rays into the wind. Hence, conditions may be achieved where the two portions of the beam are almost exactly superposed which results in a factor of 2 enhancement in the power density delivered to a target. The results depicted in Figs. 4-5 approach this ideal situation: the iso-irradiance contours show that a large fraction of the available laser power is concentrated in the upwind half of what would be an un-bloomed beam distribution.

The results presented in Figs. 2-5 would approximately correspond to the irradiance patterns, at 3 km, of a 1 MW (time average) collimated Gaussian laser beam of e-folding diameter (irradiance profile) equal to 60 cm. The environmental conditions would be: sea level, absorption coefficient equal to 0.17 km^{-1} and a lateral wind velocity equal to 10 m/s.

In summary, Figs. 2-5 show that multipulse thermal blooming may create favourable conditions of application leading to an intensification of power density on the target which are worth investigating.

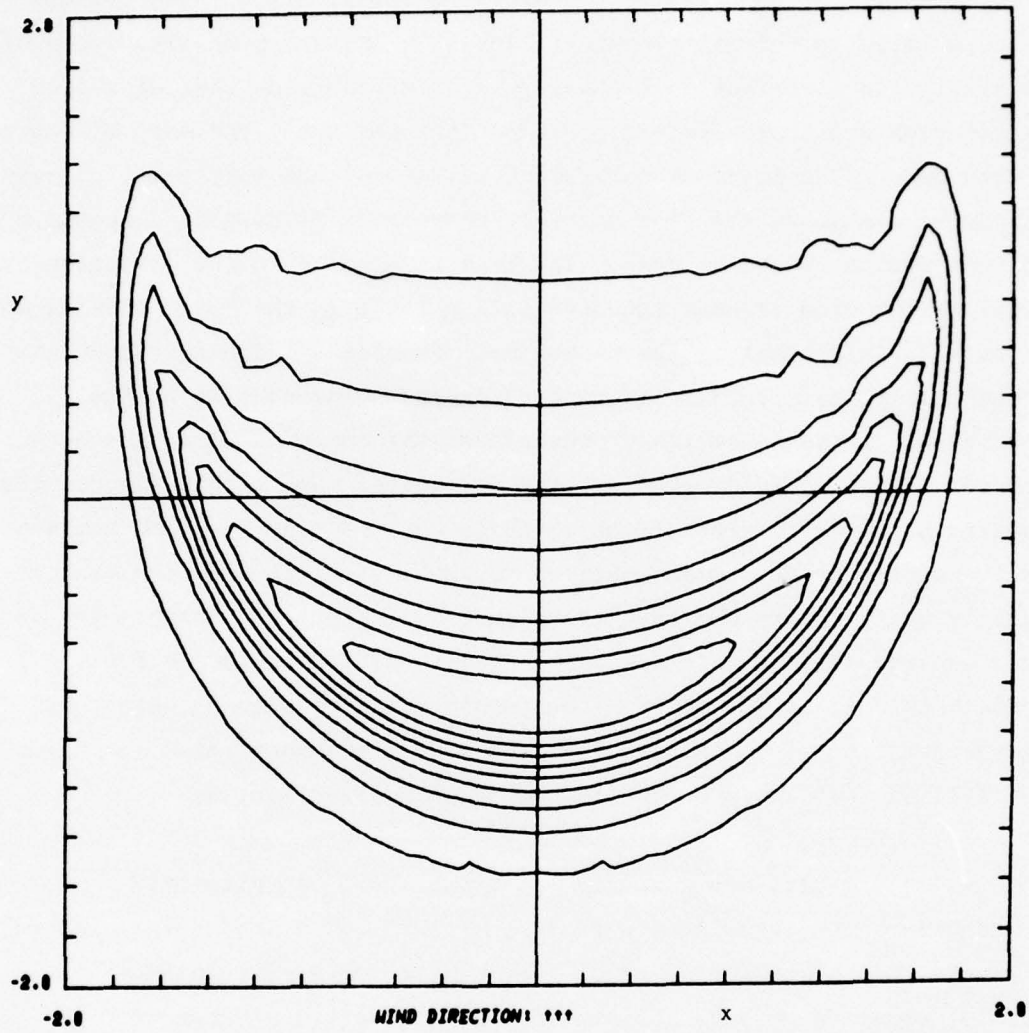

FIGURE 2 - Iso-irradiance contour lines of the computed beam irradiance pattern at $\eta = 1.15$ for $F = 20$, $\gamma = 0.45$ and $\kappa = 0$ (cw). The irradiance levels are defined by steps of 0.1 between 0.1 and 0.9 times the peak irradiance.

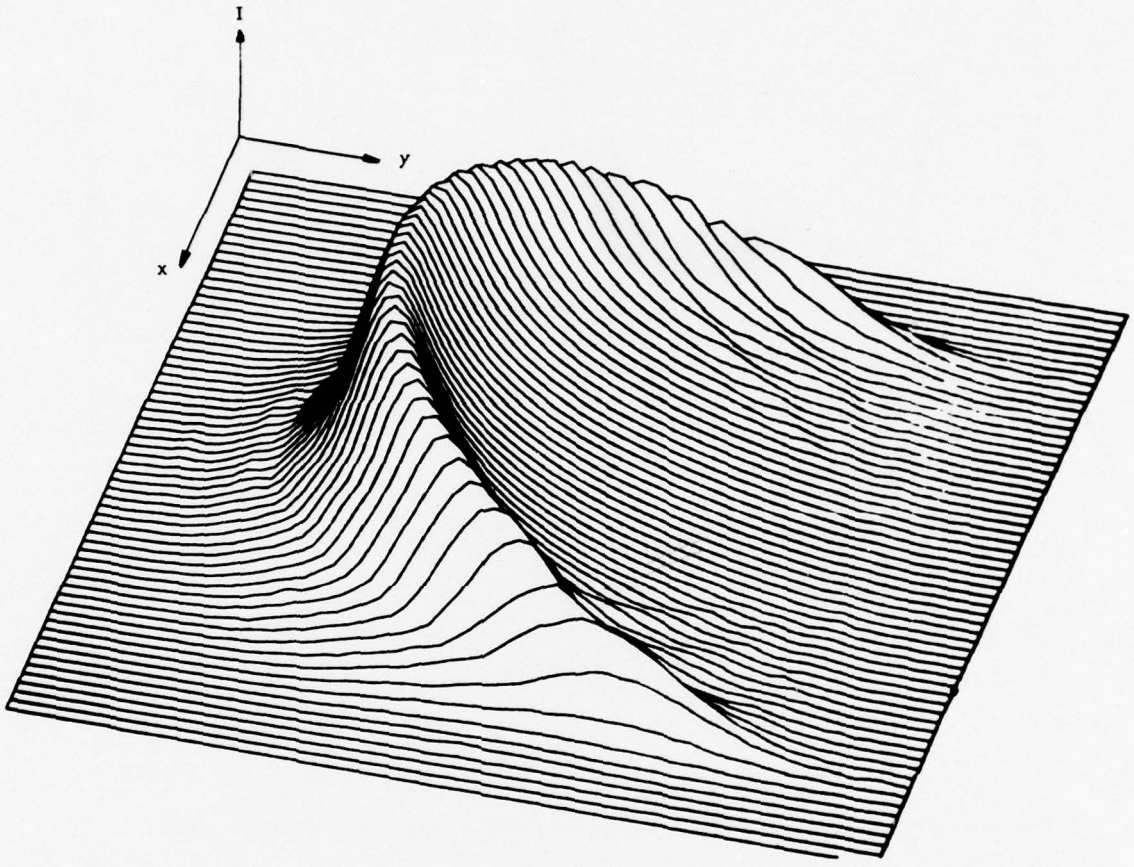

FIGURE 3 - Computed beam irradiance profile at η = 1.15 for F = 20, γ = 0.45 and κ = 0 (cw).

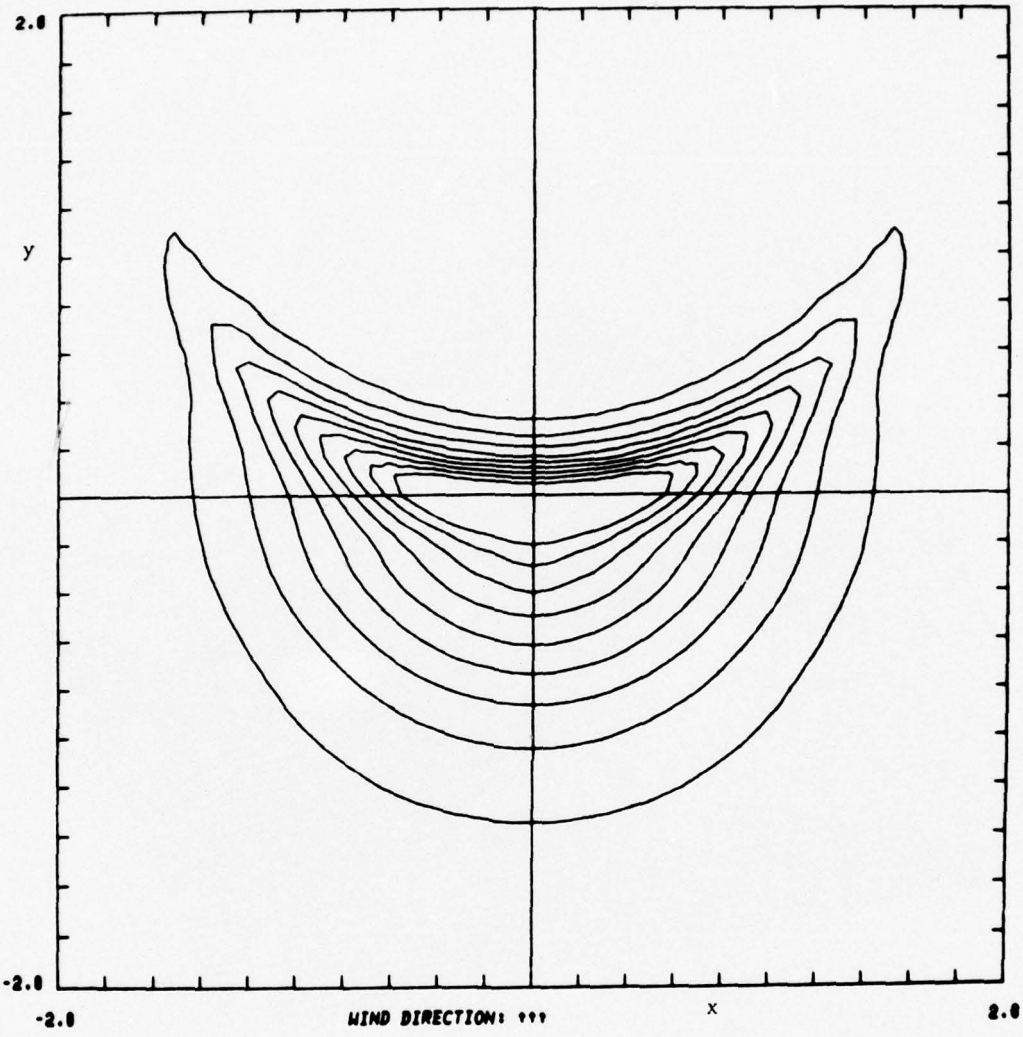

FIGURE 4 - Iso-irradiance contour lines of the computed beam irradiance pattern at $\eta = 1.12$ for $F = 20$, $\gamma = 0.45$ and $\kappa = 0.8$ (multipulse). See Fig. 2 for a definition of the irradiance levels.

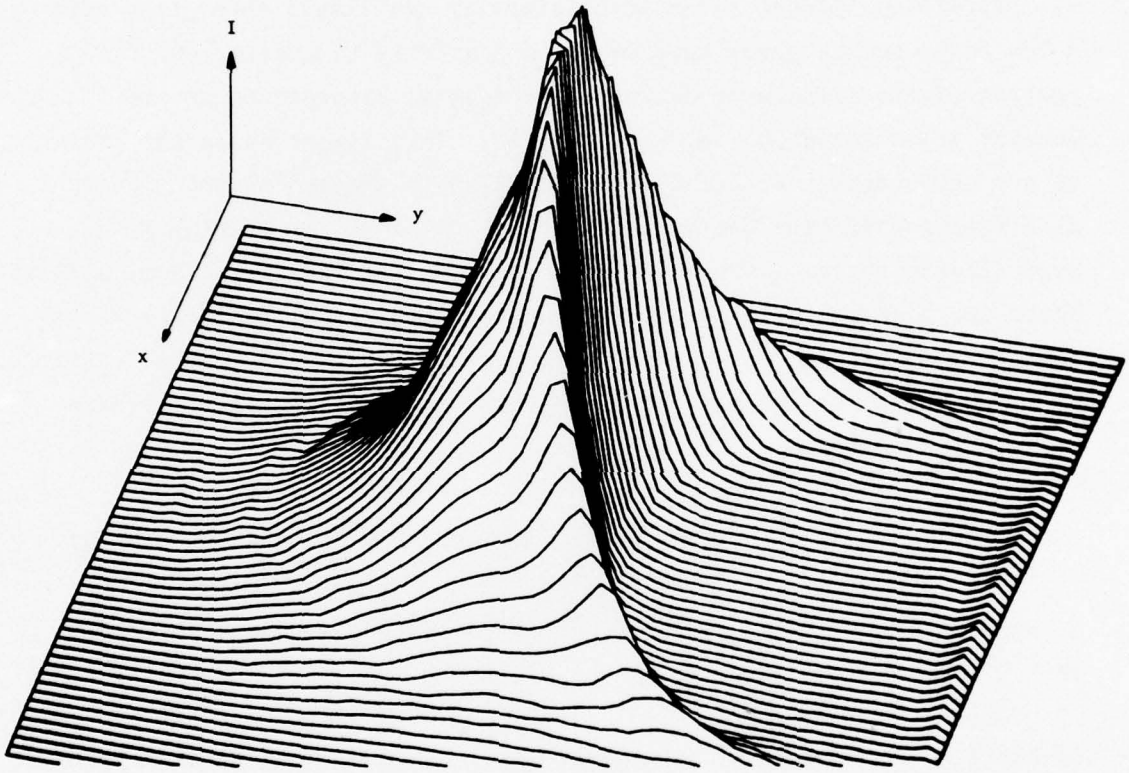

FIGURE 5 - Computed beam irradiance profile at $\eta = 1.12$ for F = 20, $\gamma = 0.45$ and $\kappa = 0.8$ (multipulse).

4.1 Experimental Verification

Very few experimental data on multipulse thermal blooming are yet available. The only direct measurements known to the author were performed in a simulation experiment conducted by Buser and co-workers (Ref. 13). A train of pulses from a TEA-CO_2 laser (typically 0.5 J/pulse) was propagated through a 1-m long laterally translated absorption cell. A low power cw-CO_2 probe beam was used coaxially to monitor the distortion of the irradiance pattern. Of special interest to us are the results illustrated in Fig. 9 of Ref. 13. This figure shows the evolution of the probe beam peak irradiance, relative to the non-blooming case, as a function of time following the first pulse of the collinear repetitively pulsed laser beam. The data run for the first three pulses. Given the conditions of application, especially $\kappa = 0.69$, steady state should be approximately attained after two pulses. The measured relative peak irradiance at the time of firing of the third pulse is somewhere between 1.30 and 1.35.

Exact numerical modelling of the experiment described in the preceding paragraph is not possible with the present version of the program. This is so because the absorbing medium in that experiment is pure CO_2 at a pressure of 7 atm which saturates at the high peak power of the multipulse beam but does not at the low power of the cw probe beam which is actually used to make the measurements. The unsaturated absorption coefficient is 0.42 m^{-1} and the extinction coefficient of the multipulse TEA laser is 0.22 m^{-1}. Therefore, the differences are significant. However, we can account for this effect in the following approximate manner. In the calculation of the scaling length ℓ_p and of the similarity parameter F, we use the unsaturated value of the absorption coefficient since, at $\kappa = 0.69$, the contribution to thermal blooming deformation comes mainly from absorption on the wings of the beam where saturation does not occur or is less pronounced. But, to evaluate the absorption number γ, we use the saturated coefficient since this number is related to linear

depletion from which the value of 0.22 m^{-1} was determined. We thus obtain for the conditions of Fig. 9 of Ref. 13 the following values for the similarity parameters:

$$\kappa = 0.69 ,$$

$$\gamma \simeq 0.35 ,$$

$$F \simeq 3.91 ,$$

and the data are reported for $\eta \simeq 0.63$. If these numbers are used in the computer program, we find for the relative steady state peak irradiance of the probe beam at $\eta = 0.63$, just prior to the firing of a pulse from the TEA laser, a value equal to 1.35. Therefore, the agreement with the reported data is almost exact. This excellent agreement is very gratifying when compared with results of other workers. For example, it is found in Ref. 13 that the relative peak irradiance intensification predicted by the numerical code of Ref. 11 is about 50% smaller than the experimental one.

4.2 Parametric Study

In view of the predicted multipulse thermal blooming enhancement shown in Figs. 2-5 which is confirmed experimentally by the data of Ref. 13, it is important to examine the dependence of the resulting intensification upon the similarity parameters κ, F and γ. This constitutes the most practical way of defining optimal operating conditions.

A simple measure of beam quality is provided by the relative time average peak irradiance. The adjective relative is used in this document to designate normalization of a variable with respect to the same variable calculated from the linearly absorbed but un-bloomed irradiance pattern. The relative, steady state, time average peak irradiance is plotted in Fig. 6 as a function of the displacement number κ for a fixed Fresnel number F = 20 and a

fixed absorption number $\gamma = 0.45$. Four curves are presented corresponding to four non-dimensional propagation distances $\eta = 0.4$, 0.8, 1.0 and 1.1 respectively. All curves are shown to pass through a maximum point for a value of κ located somewhere between 0.7 and 0.9. Fig. 7 illustrates the same results for a different choice of F and γ, namely $F = 50$ and $\gamma = 0.2$. Qualitatively, the curves shown in both figures resemble one another very closely except that the enhancement is generally higher for the conditions of Fig. 7. Optimal peak irradiance intensification at $\eta = 1.1$ is as large as 95% for $F = 50$, $\gamma = 0.2$ and 85% for $F = 20$, $\gamma = 0.45$. The optimum displacement number in all instances is approximately $\kappa = 0.8$. Therefore, it can be stated as a first conclusion that positive or favourable steady-state thermal lensing can be expected in almost all operating conditions if the repetition rate is chosen to give $\kappa \simeq 0.8$.

Since $\kappa \simeq 0.8$ represents optimal intensification, it is interesting to study how the latter varies with respect to F and γ. The relative peak irradiance at ranges of $\eta = 0.4$, 0.8, 1.0 and 1.1 is plotted in Fig. 8 versus Fresnel number for $\kappa = 0.8$ and $\gamma = 0.2$. Intensification steadily increases with F until $F \simeq 20$, where it passes through a maximum point at the longer propagation distances, and then settles to what appears to be a nearly constant value for $F \gtrsim 30$. Therefore, at propagation ranges near $\eta = 1$, Fig. 8 reveals the existence of an optimal Fresnel number whose value is slightly greater than 20; for example, the curve $\eta = 1.1$ shows a peak irradiance intensification greater than 100% for $20 \lesssim F \lesssim 30$. Finally, there remains to examine how the intensification under the most favourable conditions defined by $\kappa \simeq 0.8$ and $F \simeq 20$ changes with the third and last similarity parameter γ. This is done in Fig. 9 which shows that the optimal gain slowly decreases with increasing γ for $\eta = 1.0$ and 1.1 but remains nearly constant for $\eta = 0.4$ and 0.8. The largest drop in intensification is only 20% over γ ranging from 0.1 to 1.0. Hence, it appears that the relative optimal peak irradiance is only slightly affected by linear absorption. This result is very interesting since the absorption

number γ is the one parameter that cannot be controlled once the operating wavelength or wavelengths have been chosen.

Although the time average peak value of the transverse irradiance distribution constitutes a reasonably useful criterion to appraise the beam quality, it gives insufficient information since the thermally bloomed beam has a very complex and non-self-similar geometry. However, this deficiency can be avoided by measuring the beam quality in terms of the time-space average irradiance, denoted $\langle I \rangle_{t-s}$, over the area of the transverse plane which intercepts a given fraction of the total available power. To compute this spatial average, we need to calculate the area delimited by the iso-irradiance lines of the irradiance pattern as those illustrated in Figs. 2 and 4. A computer program was written that routinely performs this calculation for an arbitrary number of iso-irradiance contour lines of arbitrary shape. The spatial averaging inside the N^{th} level contour line is simply done as follows:

$$\langle I \rangle_{t-s}^{N} = \frac{1}{2S^{N}} \sum_{i=1}^{N} [\langle I \rangle_{t}^{i} + \langle I \rangle_{t}^{i-1}] [S^{i} - S^{i-1}], \tag{29}$$

where S^{i} designates the area bounded by the i^{th} contour curve and $\langle I \rangle_{t}^{i}$ is the corresponding irradiance level; $\langle I \rangle_{t}^{0}$ is the time average peak irradiance and $S^{0} = 0$. The chosen irradiance levels are consecutively ordered from the highest to the lowest value. If M denotes the rank of the zero-irradiance level, the fraction f(N) of the total power which passes inside the N^{th}-level contour line is given by:

$$f(N) = \frac{S^{N} \langle I \rangle_{t-s}^{N}}{S^{M} \langle I \rangle_{t-s}^{M}} . \tag{30}$$

The results for the time-space average irradiance are presented in Figs. 10-13. The parametric analysis is performed in the same manner as in Figs. 6-9. Two series of curves are given, distinguished by a suffix a or b following the figure number. Series a and b refer respectively to the

relative time-space average irradiance over the area receiving 63% and 85% of total power. These quantities are denoted as follows: ${}_{REL}\langle I\rangle^{63\%}_{t\text{-}s}$ ${}_{REL}\langle I\rangle^{85\%}_{t\text{-}s}$, 63% representing the fraction of total power comprised within the circle of e-folding radius of a Gaussian beam and 85% being, to the nearest 5%, the fraction of total power contained inside the circle bounded by the first dark ring of the diffraction pattern of a uniformly illuminated circular aperture. These quantities are truly independent of beam shape and therefore they should constitute very practical and useful criteria of laser performance under thermal blooming distortion.

Qualitatively, the results shown in Figs. 10-13 for ${}_{REL}\langle I\rangle^{63\%}_{t\text{-}s}$ and ${}_{REL}\langle I\rangle^{85\%}_{t\text{-}s}$ are very similar to those given in Figs. 6-9 for the relative time average peak irradiance. First, there is a definite optimal displacement number κ and its value obtained from Figs. 10 and 11 is also near $\kappa = 0.8\text{-}1.0$ as it was found from the peak irradiance data. The thermal blooming enhancement of the time-space average irradiance, although smaller than for the peak irradiance, is nevertheless substantial. For example, at $\eta = 1.1$, $F = 50$ and $\gamma = 0.2$, it is better than 50% for ${}_{REL}\langle I\rangle^{63\%}_{t\text{-}s}$ and better than 40% for ${}_{REL}\langle I\rangle^{85\%}_{t\text{-}s}$. Secondly, the curves of constant η in Figs. 12a and 12b show that the time-space average irradiance gain monotonically increases with Fresnel number F before reaching a constant asymptotic value. Therefore, there is no clear maximum as previously observed in Fig. 8 with regard to the relative peak irradiance, but one can still define a favourable Fresnel number range. Indeed, examination of Figs. 13a and 13b reveals that $F \gtrsim 20$ ensures optimal thermal blooming gain for propagation distances $\eta \leq 1.1$. Finally, Figs. 13a and 13b show, as before, that the absorption number γ has only a mild influence on multipulse thermal blooming intensification.

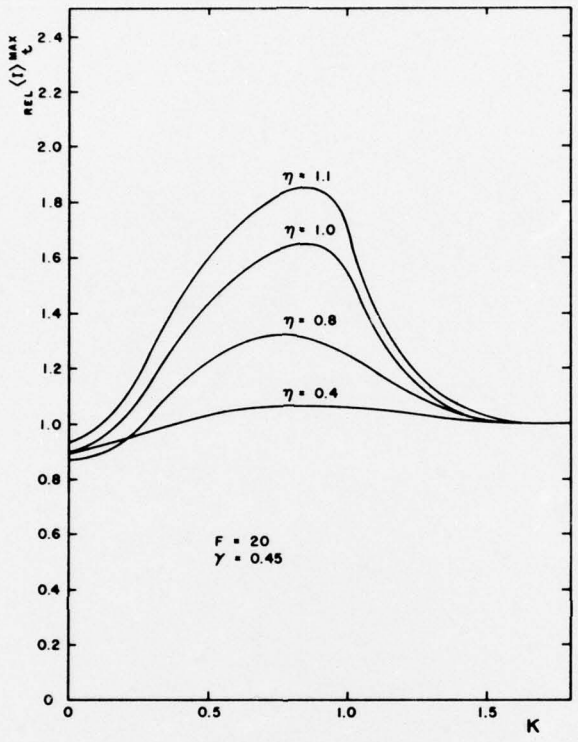

FIGURE 6 - Relative maximum values of the irradiance profiles at distances $\eta = 0.4, 0.8, 1.0$ and 1.1 as functions of similarity parameter κ for fixed $F = 20$ and $\gamma = 0.45$. Relative refers to the irradiance distribution of the un-bloomed but linearly absorbed beam.

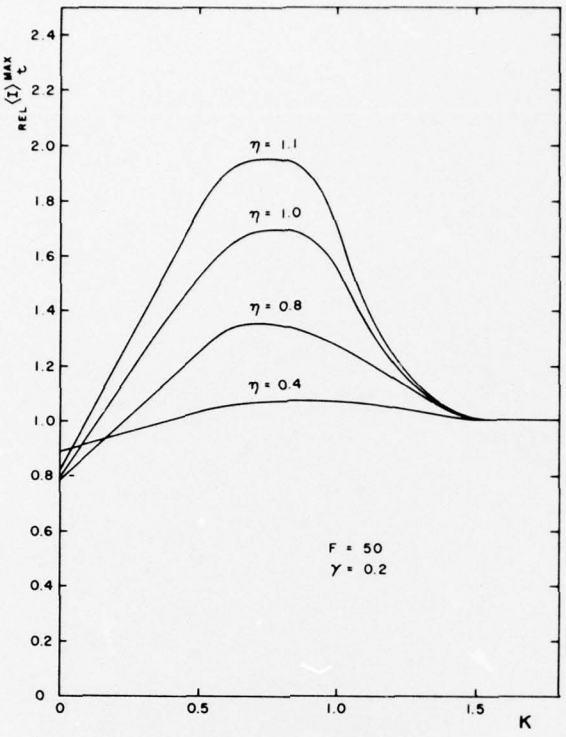

FIGURE 7 - Relative maximum values of the irradiance profiles at distances η = 0.4, 1.8, 1.0 and 1.1 as functions of similarity parameter κ for fixed F = 50 and γ = 0.2. See Fig. 6 for a definition of the term relative.

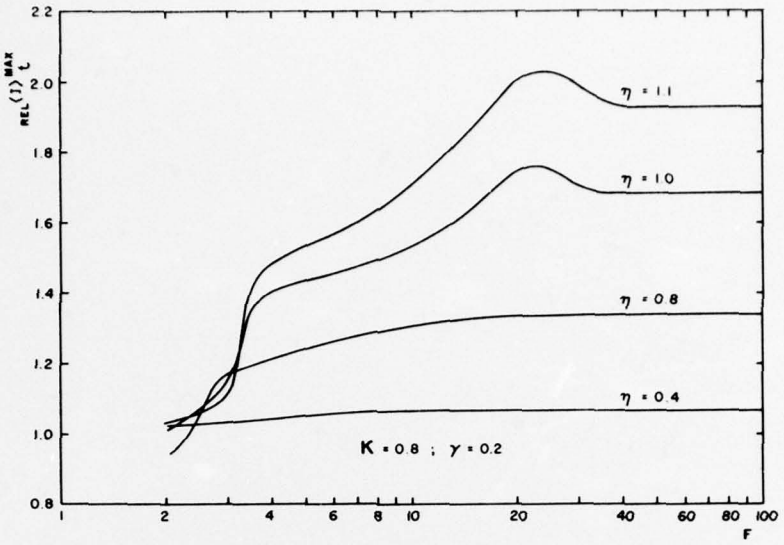

FIGURE 8 - Relative maximum values of the irradiance profiles at distances η = 0.4, 0.8, 1.0 and 1.1 as functions of similarity parameter F for fixed κ = 0.8 and γ = 0.2. See Fig. 6 for a definition of the term relative.

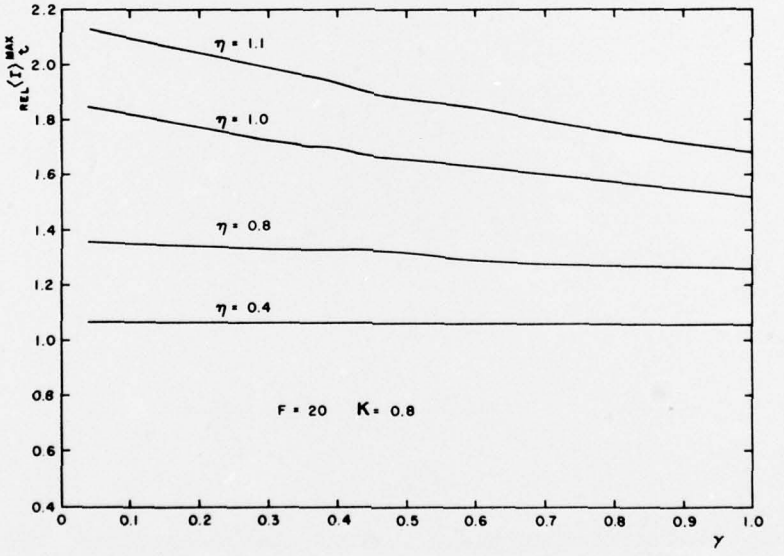

FIGURE 9 - Near optimal (κ = 0.8, F = 20) relative maximum values of the irradiance profiles at distances η = 0.4, 0.8, 1.0 and 1.1 as functions of similarity parameter γ. See Fig. 6 for a definition of the term relative.

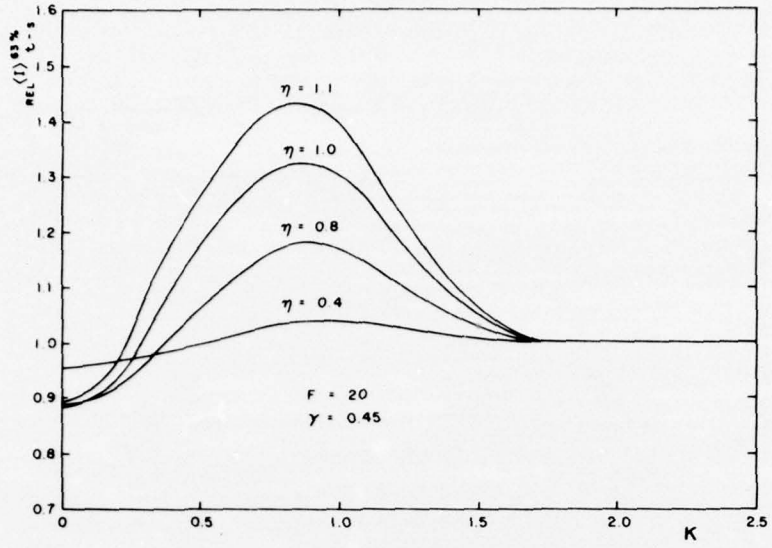

(a)

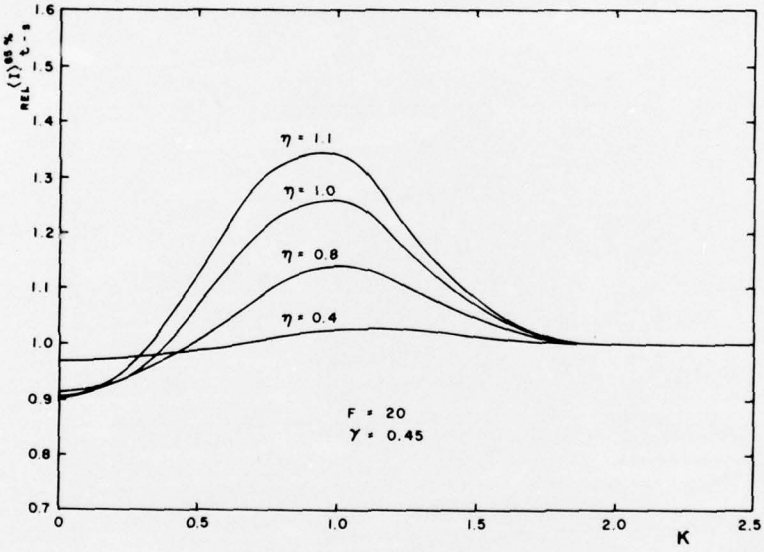

(b)

FIGURE 10 - Relative time-space average power densities, over the target area receiving 63% (a) and 85% (b) of total power at distances η = 0.4, 0.8, 1.0 and 1.1, as functions of similarity parameter κ for fixed F = 20 and γ = 0.45. See Fig. 6 for a definition of the term relative.

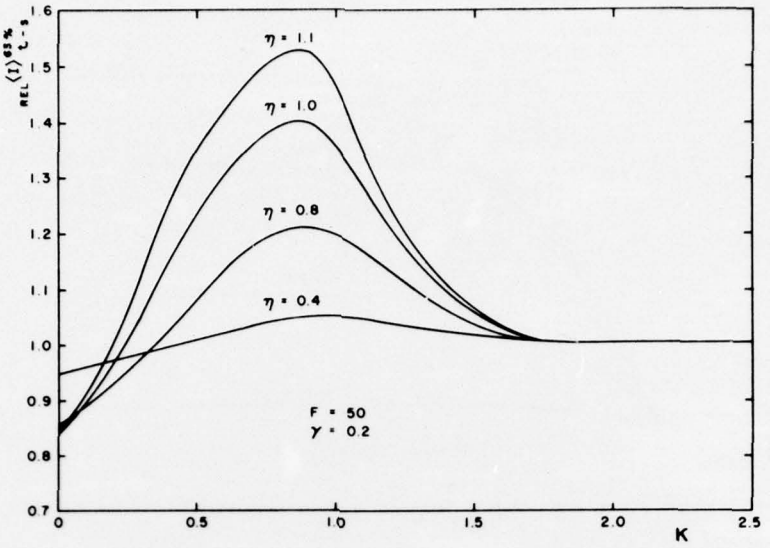

(a)

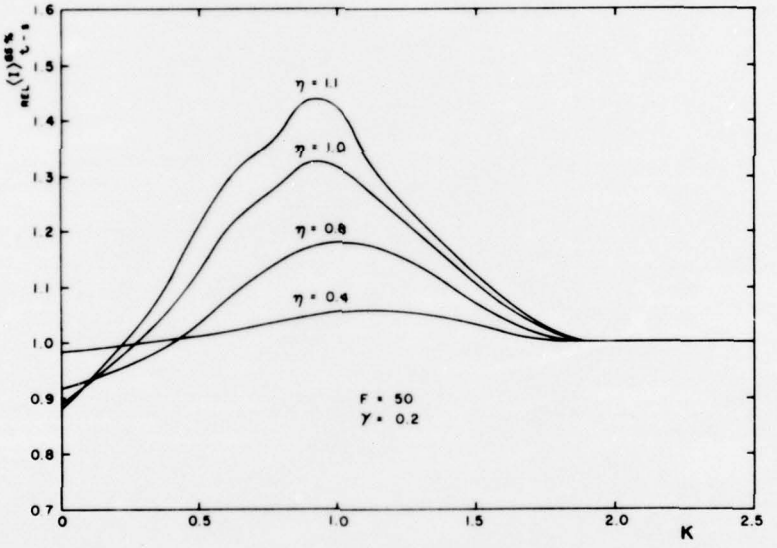

(b)

FIGURE 11 - Relative time-space average power densities, over the target area receiving 63% (a) and 85% (b) of total power at distances η = 0.4, 0.8, 1.0 and 1.1, as functions of similarity parameter κ for fixed F = 50 and γ = 0.2. See Fig. 6 for a definition of the term relative.

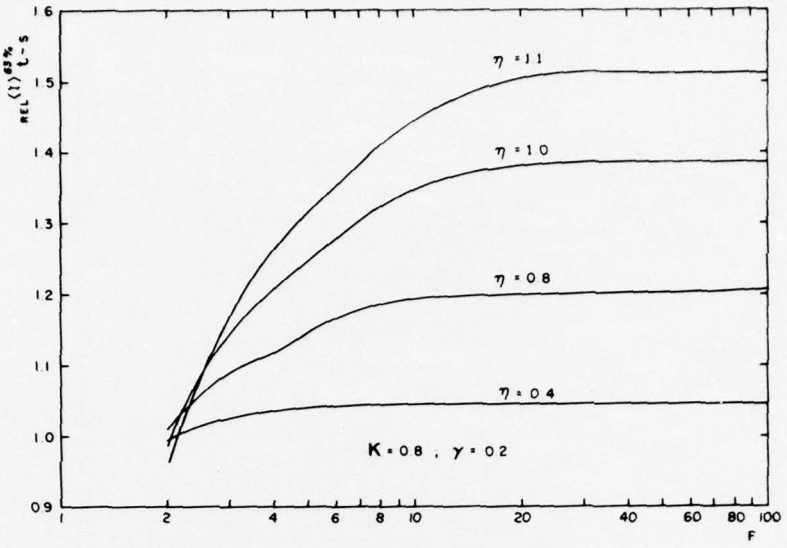

(a)

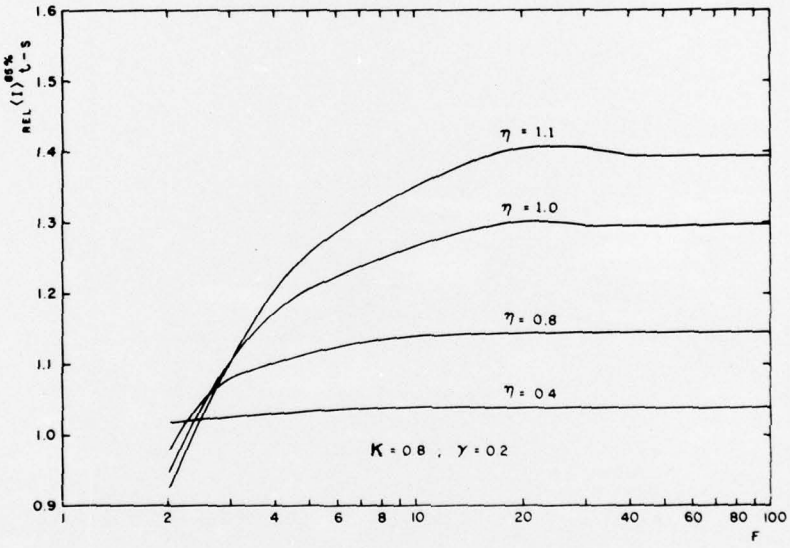

(b)

FIGURE 12 - Relative time-space average power densities, over the target area receiving 63% (a) and 85% (b) of total power at distances η = 0.4, 0.8, 1.0 and 1.1, as functions of similarity parameter F for fixed κ = 0.8 and γ = 0.2. See Fig. 6 for a definition of the term relative.

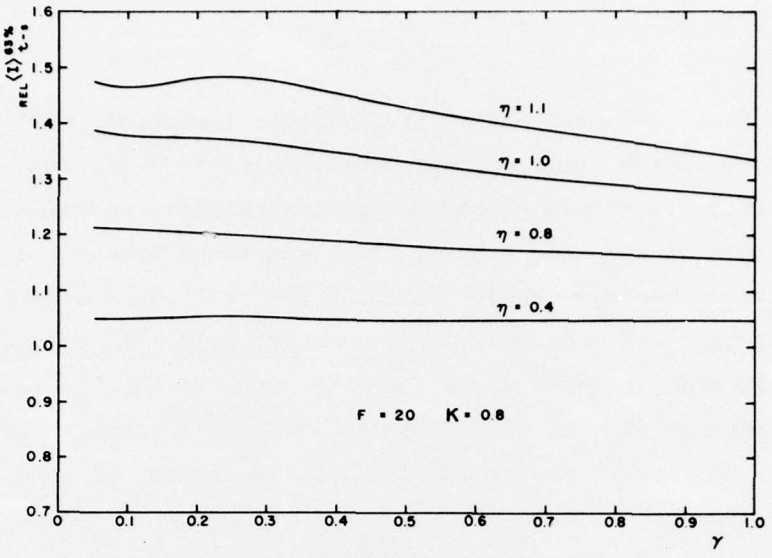

(a)

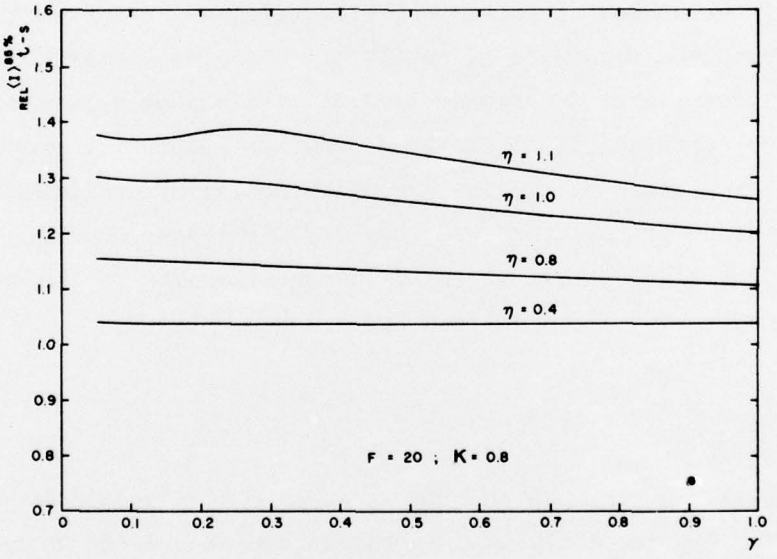

(b)

FIGURE 13 - Near optimal (κ = 0.8, F = 20) relative time-space average power densities, over the target area receiving 63% (a) and 85% (b) of total power at distances η = 0.4, 0.8, 1.0 and 1.1, as functions of similarity parameter γ. See Fig. 6 for a definition of the term relative.

5.0 CONCLUSIONS

Numerical calculations of steady state irradiance distributions of repetitively pulsed, high average power, collimated Gaussian laser beams show that multipulse thermal blooming can constitute a positive lens. Intensifications of the time average peak irradiance better than 100% and of the time-space average irradiance (over the area containing 85% of total power) better than 40% were demonstrated numerically. These numbers are at least twice as high as those quoted by other workers (Refs. 5 and 13) but available experimental data (Ref. 13) confirm almost exactly our predictions whereas those of Ref. 11 (as reported in Fig. 9 of Ref. 13) are too low by approximately the same factor of two.

A dimensional analysis of the governing equations has yielded three similarity parameters: 1) the displacement number κ which is the reciprocal of the number of pulses per flow time, 2) the Fresnel number F which measures the magnitude of cw thermal blooming distortion with respect to diffractional divergence, and 3) the number γ related to linear power losses by absorption. These three numbers completely specify the problem of steady state multipulse thermal blooming of collimated beams. A parametric study of computer solutions for collimated Gaussian beams has demonstrated that optimal intensified power density on the target can be obtained under conditions defined by:

$$0.8 \lesssim \kappa \lesssim 1.0 \ , \quad \text{and}$$

$$F \gtrsim 20$$

The remaining parameter γ has no optimal range but it should be chosen as small as possible both to minimize linear absorption and to increase thermal blooming intensification. However, its influence on the latter phenomenon (F, κ and η being the same) is rather mild.

These conclusions reveal a favourable or advantageous aspect of thermal blooming in the form of multipulse rather than cw operation which certainly must be included in the design of high-power military laser systems.

Of course, this report examines only one aspect of the problem; abstraction was made of technical feasibility and of other linear and non-linear effects. To mention only the most important, these effects are particle scattering, platform jitter, atmospheric turbulence, single-pulse thermal blooming and gas breakdown. Some of these effects are in competition. For example, pulse duration should be chosen short enough to avoid adverse single-pulse thermal blooming but, at the same time, long enough to prevent gas breakdown. Ref. 5 studies the interrelation of all these propagation phenomena in the light of a simplified empirical model, but additional work is still required to account for all effects in a more general and precise manner. Our immediate plans at DREV are to incorporate the scintillation effects of turbulence in the computer algorithm.

6.0 ACKNOWLEDGEMENTS

The author gratefully acknowledges the able assistance of Mr. P. Guay who was responsible for running the computer programs for prediction and analysis. Special thanks are also addressed to Mr. A. Blanchard of Data Systems Division who developed the basic algorithms to compute the iso-irradiance contour lines and to plot the irradiance function in isometric projection.

7.0 REFERENCES

1. Shkarofsky, I.P. and Ghosh, A.K., "Interaction of High Power Laser Beams with Matter", RCA Research Report FXC09-1, August 1973. UNCLASSIFIED

2. Hayes, John N., "Propagation of High Power Laser Beams Through the Atmosphere; an Overview", paper No. 29, AGARD Conference Proceedings No. 183 on Optical Propagation in the Atmosphere, October 1975. UNCLASSIFIED

3. Ulrich, Peter B., "Numerical Methods in High Power Laser Propagation", paper No. 31, AGARD Conference Proceedings No. 183 on Optical Propagation in the Atmosphere, October 1975. UNCLASSIFIED

4. Edelberg, S., "An Overview of the Limitations on the Transmission of High Energy Laser Beams Through the Atmosphere by Nonlinear Effects", paper No. 30, AGARD Conference Proceedings No. 183 on Optical Propagation in the Atmosphere, October 1975. UNCLASSIFIED

5. Gebhardt, Frederick G., "High Power Laser Propagation", Appl. Opt., Vol. 15, No. 6, pp 1479-1493, June 1976. UNCLASSIFIED

6. Bissonnette, L.R., "The Effect of Absorption on the Propagation of High Average Power Laser Beams", DREV M-2181/72, February 1972. UNCLASSIFIED

7. Bissonnette, L.R., "A Study of the Thermally Induced Nonlinear Propagation of a Laser Beam in an Absorbing Fluid Medium", DREV TN-2049/72, November 1972; also published in Appl. Opt., Vol. 12, No. 4, pp. 719-728, April 1973. UNCLASSIFIED

8. Bissonnette, L.R., "Déformation par l'atmosphère des faisceaux laser intenses à 10.6 μm", DREV TN-2099/74, March 1974. UNCLASSIFIED

9. Bissonnette, L.R. and Rioux, M.-A., "Experiments on Simulated Self-Induced Thermal Distortion of Laser Beams", DREV R-2125/74, October 1974. UNCLASSIFIED.

10. Rossignol, O., "Simulation numérique de la défocalisation thermique d'un faisceau laser intense", DREV R-4029/76, February 1976. UNCLASSIFIED

11. Wallace, James and Lilly Julius Q., "Thermal Blooming of Repetitively Pulsed Laser Beams", J. Opt. Soc. Am., Vol. No. 64, No. 12, pp. 1651-1655, December 1974. UNCLASSIFIED

12. Wallace, James and Pasciak, Joseph, "Compensating for Thermal Blooming of Repetitively Pulsed Lasers", J. Opt. Soc. Am., Vol. 65, No. 11, pp. 1257-1260, November 1975. UNCLASSIFIED

13. Buser, R.G., Rohde, R.S., Berger, P.J., Gebhardt, F.G. and Smith, D.C., "Transient Thermal Blooming of Single and Multiple Short Laser Pulses", Appl. Opt., Vol. 14, No. 11, pp. 2740-2746, November 1975. UNCLASSIFIED

14. Richtmyer, Robert D. and Morton, K.W., "Difference Methods for Initial-Value Problems", Interscience Publishers, New York 1957. UNCLASSIFIED

DREV REPORT 4067/77 (UNCLASSIFIED)

Bureau - Recherche et Développement, Ministère de la Défense nationale, Canada.
CRDV, C.P. 880, Courcelette, Qué. GOA 1RO.

"Steady State Thermal Blooming of Multipulse Laser Beams"
by L.R. Bissonnette

On étudie, à l'aide de solutions numériques, l'état stationnaire de la défocalisation thermique d'un faisceau laser à impulsions multiples soumis à un vent latéral. On trouve, pour un taux d'impulsions favorable, une augmentation de 100% de l'intensité maximale par rapport au faisceau qui se propagerait sans déformation mais avec absorption linéaire. La valeur correspondante du gain exprimé en terme de l'intensité moyenne sur la surface de la cible qui reçoit 85% de la puissance totale est de 40%. Trois paramètres de similitude suffisent pour définir complètement le problème: le nombre κ qui est égal à la réciproque du nombre d'impulsions transmises pendant le temps de transit de l'air dans le faisceau, le nombre de Fresnel F basé sur la longueur caractéristique de l'interaction absorption-intensité et le nombre γ relié à l'absorption linéaire. Une étude paramétrique en fonction de ces trois paramètres démontre que des conditions optimales de gain dans le cas d'un faisceau gaussien collimaté existent pour: $0.8 \le \kappa \le 1.0$ et $F \ge 20$. L'amplification décroît généralement avec l'accroissement de γ mais de façon peu sensible.

DREV REPORT 4067/77 (UNCLASSIFIED)

Bureau - Recherche et Développement, Ministère de la Défense nationale, Canada.
CRDV, C.P. 880, Courcelette, Qué. GOA 1RO.

"Steady State Thermal Blooming of Multipulse Laser Beams"
by L.R. Bissonnette

On étudie, à l'aide de solutions numériques, l'état stationnaire de la défocalisation thermique d'un faisceau laser à impulsions multiples soumis à un vent latéral. On trouve, pour un taux d'impulsions favorable, une augmentation de 100% de l'intensité maximale par rapport au faisceau qui se propagerait sans déformation mais avec absorption linéaire. La valeur correspondante du gain exprimé en terme de l'intensité moyenne sur la surface de la cible qui reçoit 85% de la puissance totale est de 40%. Trois paramètres de similitude suffisent pour définir complètement le problème: le nombre κ qui est égal à la réciproque du nombre d'impulsions transmises pendant le temps de transit de l'air dans le faisceau, le nombre de Fresnel F basé sur la longueur caractéristique de l'interaction absorption-intensité et le nombre γ relié à l'absorption linéaire. Une étude paramétrique en fonction de ces trois paramètres démontre que des conditions optimales de gain dans le cas d'un faisceau gaussien collimaté existent pour: $0.8 \le \kappa \le 1.0$ et $F \ge 20$. L'amplification décroît généralement avec l'accroissement de γ mais de façon peu sensible.

DREV REPORT 4067/77 (UNCLASSIFIED)

Bureau - Recherche et Développement, Ministère de la Défense nationale, Canada.
CRDV, C.P. 880, Courcelette, Qué. GOA 1RO.

"Steady State Thermal Blooming of Multipulse Laser Beams"
by L.R. Bissonnette

On étudie, à l'aide de solutions numériques, l'état stationnaire de la défocalisation thermique d'un faisceau laser à impulsions multiples soumis à un vent latéral. On trouve, pour un taux d'impulsions favorable, une augmentation de 100% de l'intensité maximale par rapport au faisceau qui se propagerait sans déformation mais avec absorption linéaire. La valeur correspondante du gain exprimé en terme de l'intensité moyenne sur la surface de la cible qui reçoit 85% de la puissance totale est de 40%. Trois paramètres de similitude suffisent pour définir complètement le problème: le nombre κ qui est égal à la réciproque du nombre d'impulsions transmises pendant le temps de transit de l'air dans le faisceau, le nombre de Fresnel F basé sur la longueur caractéristique de l'interaction absorption-intensité et le nombre γ relié à l'absorption linéaire. Une étude paramétrique en fonction de ces trois paramètres démontre que des conditions optimales de gain dans le cas d'un faisceau gaussien collimaté existent pour: $0.8 \le \kappa \le 1.0$ et $F \ge 20$. L'amplification décroît généralement avec l'accroissement de γ mais de façon peu sensible.

DREV REPORT 4067/77 (UNCLASSIFIED)

Bureau - Recherche et Développement, Ministère de la Défense nationale, Canada.
CRDV, C.P. 880, Courcelette, Qué. GOA 1RO.

"Steady State Thermal Blooming of Multipulse Laser Beams"
by L.R. Bissonnette

On étudie, à l'aide de solutions numériques, l'état stationnaire de la défocalisation thermique d'un faisceau laser à impulsions multiples soumis à un vent latéral. On trouve, pour un taux d'impulsions favorable, une augmentation de 100% de l'intensité maximale par rapport au faisceau qui se propagerait sans déformation mais avec absorption linéaire. La valeur correspondante du gain exprimé en terme de l'intensité moyenne sur la surface de la cible qui reçoit 85% de la puissance totale est de 40%. Trois paramètres de similitude suffisent pour définir complètement le problème: le nombre κ qui est égal à la réciproque du nombre d'impulsions transmises pendant le temps de transit de l'air dans le faisceau, le nombre de Fresnel F basé sur la longueur caractéristique de l'interaction absorption-intensité et le nombre γ relié à l'absorption linéaire. Une étude paramétrique en fonction de ces trois paramètres démontre que des conditions optimales de gain dans le cas d'un faisceau gaussien collimaté existent pour: $0.8 \le \kappa \le 1.0$ et $F \ge 20$. L'amplification décroît généralement avec l'accroissement de γ mais de façon peu sensible.

DREV REPORT 4067/77 (UNCLASSIFIED)

Research and Development Branch, Department of National Defence, Canada.
DREV, P.O. Box 880, Courcelette, Que. G0A 1R0.

"Steady State Thermal Blooming of Multiple Laser Beams"
by L.R. Bissonnette

Steady state thermal blooming of multipulse laser beams subjected to cross winds is studied in the light of numerical solutions. Enhancement resulting in a 100% increase of the peak irradiance with respect to the non-bloomed but linearly absorbed beam is demonstrated at the optimal pulsing rate. The corresponding gain in terms of spatially averaged power density over the target area containing 85% of total power is 40%. A parametric study is made as a function of three similarity parameters which are sufficient to completely define the problem: the number κ which is the reciprocal of the number of pulses per flow time, the Fresnel number F based on the absorption-irradiance interaction length scale and the absorption number γ related to linear depletion. Optimal conditions for a collimated Gaussian beam are shown to exist for $0.8 \leq \kappa \leq 1.0$ and $F \geq 20$. Intensification generally decreases with increasing γ but only slightly.

DREV REPORT 4067/77 (UNCLASSIFIED)

Research and Development Branch, Department of National Defence, Canada.
DREV, P.O. Box 880, Courcelette, Que. G0A 1R0.

"Steady State Thermal Blooming of Multiple Laser Beams"
by L.R. Bissonnette

Steady state thermal blooming of multipulse laser beams subjected to cross winds is studied in the light of numerical solutions. Enhancement resulting in a 100% increase of the peak irradiance with respect to the non-bloomed but linearly absorbed beam is demonstrated at the optimal pulsing rate. The corresponding gain in terms of spatially averaged power density over the target area containing 85% of total power is 40%. A parametric study is made as a function of three similarity parameters which are sufficient to completely define the problem: the number κ which is the reciprocal of the number of pulses per flow time, the Fresnel number F based on the absorption-irradiance interaction length scale and the absorption number γ related to linear depletion. Optimal conditions for a collimated Gaussian beam are shown to exist for $0.8 \leq \kappa \leq 1.0$ and $F \geq 20$. Intensification generally decreases with increasing γ but only slightly.

DREV REPORT 4067/77 (UNCLASSIFIED)

Research and Development Branch, Department of National Defence, Canada.
DREV, P.O. Box 880, Courcelette, Que. G0A 1R0.

"Steady State Thermal Blooming of Multiple Laser Beams"
by L.R. Bissonnette

Steady state thermal blooming of multipulse laser beams subjected to cross winds is studied in the light of numerical solutions. Enhancement resulting in a 100% increase of the peak irradiance with respect to the non-bloomed but linearly absorbed beam is demonstrated at the optimal pulsing rate. The corresponding gain in terms of spatially averaged power density over the target area containing 85% of total power is 40%. A parametric study is made as a function of three similarity parameters which are sufficient to completely define the problem: the number κ which is the reciprocal of the number of pulses per flow time, the Fresnel number F based on the absorption-irradiance interaction length scale and the absorption number γ related to linear depletion. Optimal conditions for a collimated Gaussian beam are shown to exist for $0.8 \leq \kappa \leq 1.0$ and $F \geq 20$. Intensification generally decreases with increasing γ but only slightly.

DREV REPORT 4067/77 (UNCLASSIFIED)

Research and Development Branch, Department of National Defence, Canada.
DREV, P.O. Box 880, Courcelette, Que. G0A 1R0.

"Steady State Thermal Blooming of Multiple Laser Beams"
by L.R. Bissonnette

Steady state thermal blooming of multipulse laser beams subjected to cross winds is studied in the light of numerical solutions. Enhancement resulting in a 100% increase of the peak irradiance with respect to the non-bloomed but linearly absorbed beam is demonstrated at the optimal pulsing rate. The corresponding gain in terms of spatially averaged power density over the target area containing 85% of total power is 40%. A parametric study is made as a function of three similarity parameters which are sufficient to completely define the problem: the number κ which is the reciprocal of the number of pulses per flow time, the Fresnel number F based on the absorption-irradiance interaction length scale and the absorption number γ related to linear depletion. Optimal conditions for a collimated Gaussian beam are shown to exist for $0.8 \leq \kappa \leq 1.0$ and $F \geq 20$. Intensification generally decreases with increasing γ but only slightly.